



Flotation behavior and adsorption mechanism of (1-hydroxy-2-methyl-2-octenyl) phosphonic acid to cassiterite

Xin TAN^{1,2}, Fa-yu HE³, Yan-bo SHANG², Wan-zhong YIN¹

1. College of Resources and Civil Engineering, Northeastern University, Shenyang 110819, China;
2. State Key Laboratory of Mineral Processing, Research & Design Institute of Mineral Engineering, Beijing General Research Institute of Mining & Metallurgy, Beijing 102628, China
3. China Minmetals Corporation, Beijing 100010, China

Received 14 October 2015; accepted 12 April 2016

Abstract: The flotation behavior and adsorption mechanism of novel (1-hydroxy-2-methyl-2-octenyl) phosphonic acid (HEPA) to cassiterite were investigated by micro-flotation tests, zeta potential measurements, FTIR determination and density functional theory (DFT) calculation. The flotation results demonstrated that HEPA exhibited superior collecting performance compared with styrene phosphonic acid (SPA). The cassiterite recovery maintained above 90% over a wide pH range of 2–9 with 50 mg/L HEPA. The results of zeta potential measurement and FTIR detection indicated that the adsorption of HEPA onto cassiterite was mainly attributed to the chemisorption between HEPA monoanions and Sn species on mineral surfaces. The DFT calculation results demonstrated that HEPA monoanions owned higher HOMO energy and exhibited a better affinity to cassiterite than SPA, which provided very clear evidence for the stronger collecting power of HEPA presented in floatation test and zeta potential measurement.

Key words: (1-hydroxy-2-methyl-2-octenyl) phosphonic acid; cassiterite; adsorption; flotation; density functional theory

1 Introduction

The first recorded cassiterite flotation was at Altenberg tin concentrator, Ore Mountains, Saxony in 1938 [1]. In the early stage, the low selectivity fatty acid products were used as collector. From the 1930s till the present time, a substantial amount of higher selectivity collectors have been reported [2–5]. However, arsonic acids which owned the highest selectivity were ceased because of their toxicity [3]; sulfosuccinamates which owned strong framing characteristics were perceived to be disadvantageous [3,6,7]; the wide application of hydroxamic acids which were high selectivity [8,9] was also limited due to the high cost. Phosphonic acids and their products were also suitable collectors for cassiterite floatation and were investigated initially as alternatives to the every toxic arsonic acids [10].

Large amounts of works on cassiterite flotation by various aryl phosphonic acids and alkyl phosphonic acids compounds have been reported [10,11]. The work concluded that styrene phosphonic acid (SPA) is the most efficient one. GRUNER and BILSING [1] used SPA as

collector to dispose many different tin ores in laboratory tests, and investigated the application of SPA in many processing plants. They suggested that SPA is an ideal flotation collector for finely disseminated cassiterite and wolframite ores, and it is possible to obtain a high-grade concentrates containing more than 40% Sn with a high recovery. 1-hydroxyalkylidene-1,1-diphosphonic acid (Flotol-7,9) with 7–9 carbon atoms was also reported to be an excellent collection property for cassiterite [12]. LI et al [13] investigated the flotation performances and adsorption mechanism of α -hydroxyoctyl phosphonic acid (HPA) to cassiterite. The experiment results indicated that HPA reacts with Sn species by formation of Sn–P and Sn–O–P bonds and shows excellent collecting ability and selectivity. In addition, phenylphosphonates and phenylphosphinics have also received much interest [12,14]. Although there were many reports about cassiterite flotation by phosphonic acid compounds, the research on structure–property relationship of phosphonic acid collectors was rare.

Computational methods such as ab initio and density functional theory (DFT) are helpful tools to investigate various chemical reactivity systems.

Especially, the DFT calculation has been known as a reliable and inexpensive method for obtaining chemical information about the energetics, structure, and properties of atoms and molecules [15–17]. It has been widely applied to analyzing and elucidating the inner mechanisms of chemical reactivity [18], structure–property relationship [19], and interface chemistry reaction [20]. The DFT calculation was also used to investigate the energetics and the relaxed ionic positions of several low-index stoichiometric cassiterite surfaces by OVIEDO and GILLAN [21].

However, the DFT research on cassiterite flotation has been rarely reported. In order to search for a more efficient phosphonic acid collector for cassiterite, and achieve the acceptable flotation performance of phosphonic acids serving as collectors in oxidized ores flotation, a novel phosphonic acid — (1-hydroxy-2-methyl-2-octenyl) phosphonic acid (HEPA) was introduced as a collector for cassiterite flotation in this work, and its flotation behavior was compared with SPA. The interaction between new surfactant and cassiterite was evaluated by FTIR detection and zeta potential measurement. Moreover, the density functional theory (DFT) calculation was adopted to infer the phosphonic acids' adsorption mechanism and structure–property relationship.

2 Experimental

2.1 Minerals and materials

Cassiterite obtained from the Geological Museum of China was dry ground to fine particles by using agate mortar and pestle. The mineral particles in the range of 0.038–0.076 mm were selected for micro-flotation experiments and the sample with particle size lower than 0.005 mm was used for FTIR measurement and zeta potential determination. The purity of mineral particles was over 96% (mass fraction) based on mineral element analysis. HEPA (>95%, mass fraction) used in this study was synthesized by our research team using the method mentioned by ALBOUY et al [22] and ZHONG et al [23]. SPA (>80%, mass fraction) were produced by LUOKE commercial chemical companies (Beijing, China) and its recrystallization product (92%, mass fraction) was used for flotation tests. Water used in all tests was distilled and all other chemicals used in this work were of analytic grade.

2.2 Micro-flotation tests

Micro-flotation tests were executed using a XFG5–35 flotation machine with a plexiglass cell of effective volume 40 mL and the impeller speed was fixed at 1680 r/min. 2.0 g pure mineral samples together with

40 mL distilled water were placed in the cell. After adding a desired amount of collector, the suspension was agitated for 3 min and the pH value was adjusted to a desired value with hydrochloric acid or sodium hydroxide solution. The flotation was conducted for 5 min. The products and tails were weighed separately after filtration and drying. The results were given in recovery (i.e., mass fraction) of mineral floated.

2.3 Zeta potential measurement

Zeta-potentials of minerals were measured by a Brookhaven zeta plus zeta potential analyzer (USA). A 0.5 g mineral sample was stirred for 5 min in a 30 mL solution with or without 50 mg/L HEPA or SPA. The pH values were adjusted to a desired one by adding sodium hydroxide or hydrochloric acid solutions. All measurements were conducted in a 0.01 mol/L KCl background electrolyte solution. The agitated suspension was sampled to record the zeta-potential. The results presented were the average of three independent measurements with a typical variation of ± 2 mV.

2.4 FTIR determination

The Fourier transform infrared spectroscopy (FTIR) determinations of products were measured by a EQUINOX 55 Fourier transform infrared spectrometer of BRUKER company at a resolution of 4 cm^{-1} using potassium bromide pellet technology. The scan scope ranged from 400 to 4000 cm^{-1} . A 0.5 g mineral sample was placed in a 100 mL conical flask, to which 50 mL 50 mg/L phosphonic acid solution was added. After stirring in $25\text{ }^{\circ}\text{C}$ for 10 min, the mineral particle was centrifuged, washed twice and dried at room temperature, and then was used for FTIR detection.

2.5 DFT calculation

All calculations were performed in Accelrys Material studio 7.0 (MS) modeling package and the geometric structure and atomic charges of products were calculated using the DMol³ module on the basis of density functional theory (DFT). The generalized gradient approximation (GGA) developed by Perdew–Burke–Ernzerhof (PBE) was used as the exchange correlation functional and double numerical plus polarization (DNP) was used as atomic orbital basis. Core treatment was all electron relativistic. The accuracy of k-point was set to be fine. Energy change per atom was less than 27.21×10^{-5} eV. Max force was less than 5.442×10^{-3} eV/Å. Max displacement of atoms during the geometry optimization was no more than 0.002 Å and SCF density convergence was less than 2.721×10^{-5} eV. The salvation model was also used with the dielectric constant for water being 78.54.

3 Results and discussion

3.1 Flotation test

The results of cassiterite flotation with HEPA and SPA as collector in the presence or absence of the frother 2# oil were shown in Fig. 1. The results indicated that HEPA showed a rapid flotation response to cassiterite, with recovery reaching above 90% in 2.5 min. In contrast, SPA presented much lower activity especially in the absence of 2# oil. The recovery attained preferable values in 5 min when SPA was used in the presence of 2# oil, while the recovery was no more than 10% without 2# oil. These results revealed that HEPA exhibited much higher activity to cassiterite than SPA.

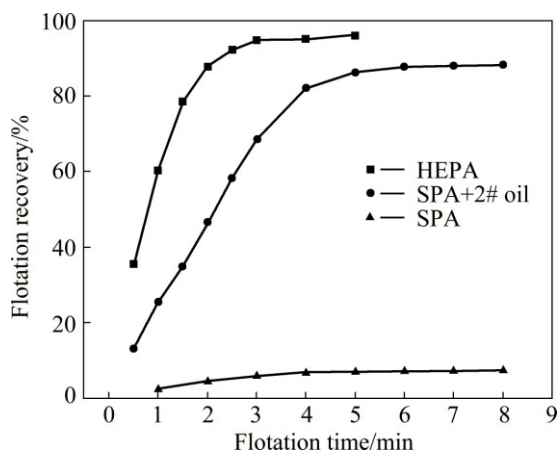


Fig. 1 Flotation recovery of cassiterite with HEPA and SPA as collector in presence or absence of frother 2# oil ($\rho_{\text{HEPA}}=50$ mg/L, $\rho_{\text{SPA}}=50$ mg/L, $\rho_{2\# \text{ oil}}=250$ mg/L, pH=4)

The effects of pH on recovery of cassiterite with collector concentration of 50 mg/L are shown in Fig. 2. As shown in Fig. 2, the recovery maintained above 90% in pH ranging from 2 to 9 when HEPA was used. However, the flotation response had a gradual decrease in pH region of 7–9 and dropped rapidly when pH value was beyond 9. The appropriate pH value for SPA was around 2–7, in this range, the recovery maintained above 80%. Both of these two collectors were unsuitable to be used in alkaline solution or strong acidic environment of pH<2. In addition, it was clear that HEPA had much stronger collecting ability than SPA since the flotation recovery of HEPA was higher than that of SPA over a wide pH range.

The effects of collector concentration on recovery of cassiterite at pH=4.0 are exhibited in Fig. 3. As shown in Fig. 3, the recovery of minerals increased with the increasing of phosphonic acids concentration. When the concentration of HEPA was greater than 20 mg/L, recovery remained above 90%. In contrast to that, the recovery maintained around 85% even if the initial

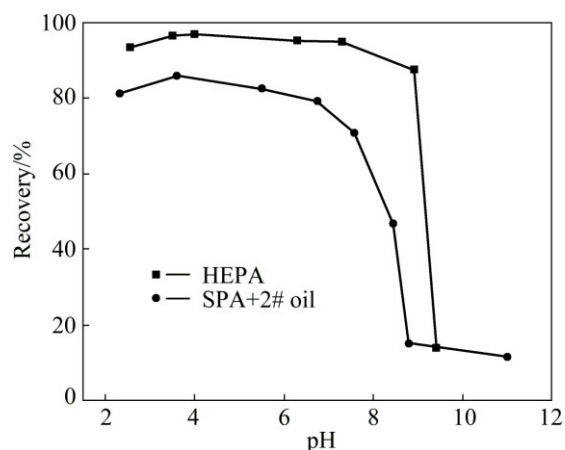


Fig. 2 Recovery of cassiterite as function of pH (collector concentration =50 mg/L)

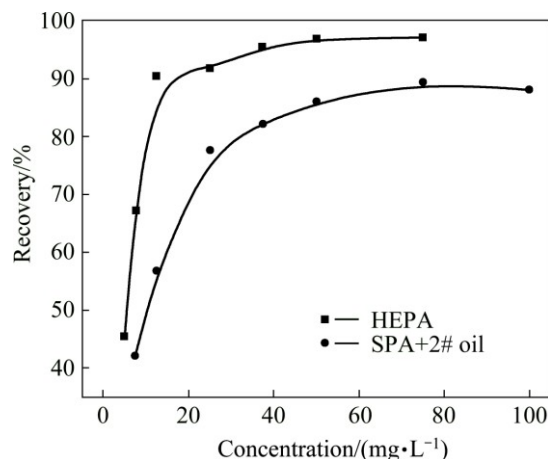


Fig. 3 Recovery of cassiterite as function of collector concentration at pH 4.0

concentration of SPA was higher than 50 mg/L. It further demonstrated that HEPA showed higher flotation efficiency than SPA.

3.2 Zeta potential measurement

Figure 4 shows the variation of the zeta potentials of cassiterite with pH values in the absence and presence of 50 mg/L collectors. As shown in Fig. 4, the isoelectric point (IEP) of cassiterite was around 3.6, which was in accordance with those previously reported [24,25]. The zeta potentials of cassiterite showed a negative shift after adding HEPA or SPA over the pH range of 3–9, indicating that these two anion collectors have adsorbed onto cassiterite surface. When pH values were above 3.6, both cassiterite and collectors were negatively charged, resulting in the fact that the adsorption of HEPA or SPA onto cassiterite surfaces had to overcome the electrostatic repulsion. The results revealed that a strong chemisorption behavior existed between those collectors and mineral surfaces.

Moreover, the negative shift of zeta potential of cassiterite in presence of HEPA was more than that in

presence of SPA, demonstrating that more HEPA collectors were attracted onto the cassiterite surfaces. Therefore, HEPA exhibited superior adsorption ability to cassiterite over SPA, which was in good agreement with the flotation performance.

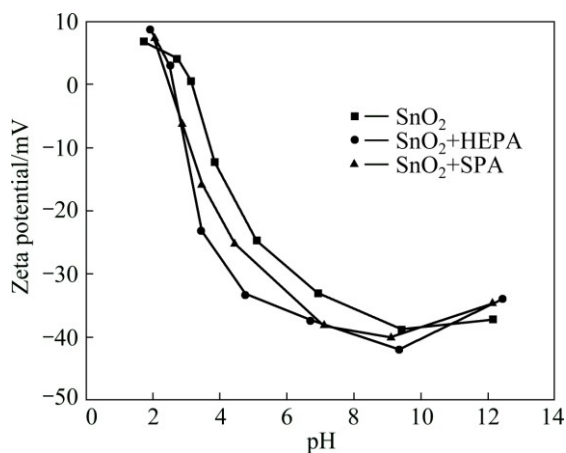


Fig. 4 Zeta potential of cassiterite as function of pH in absence and presence of 50 mg/L SPA or HEPA

3.3 FTIR determination

The FTIR spectra of cassiterite before and after interaction with HEPA or SPA (pH=4) were presented in Fig. 5. As can be seen in Fig. 5, the significant characteristic adsorption bands of cassiterite appeared at the band around 740–670 cm^{-1} and 630 cm^{-1} [26]. In addition, the bands around 3400 and 1650–1640 cm^{-1} were due to the —O—H stretching of water, and the peak around 1385 cm^{-1} may result from the presence of impurity nitrate in KBr. After interaction with phosphonic acid, cassiterite surfaces exhibited new adsorption bands at 2931 cm^{-1} and 2884 cm^{-1} , which were attributed to the stretching bands of —CH₃ and —CH₂ groups in collector molecules, demonstrating that both HEPA and SPA had adsorbed on the mineral surfaces. The phosphonic acid group was prominent in

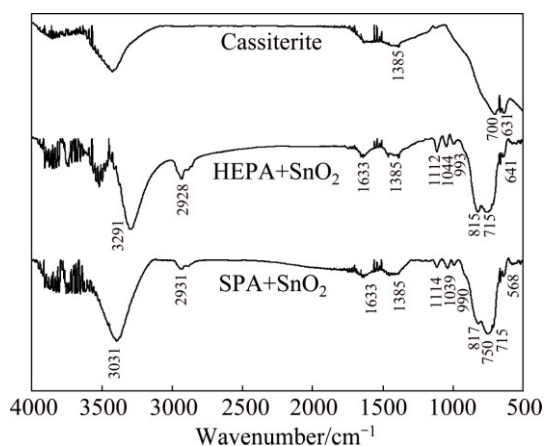
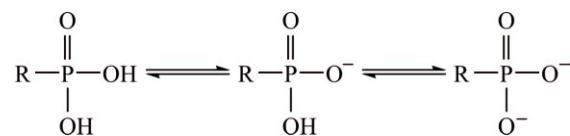


Fig. 5 FTIR spectra of cassiterite before and after interaction with HEPA or SPA (pH=4)

region of 1900–850 cm^{-1} [27]. As can be observed in this region, the new bands positioned at 1112, 1040 and 815 cm^{-1} corresponded much better with the stretching vibration of P=O bond and P—O bond [28] in Sn–SPA complex reported by KUYS and ROBERTS [27] and CHEN et al [29]. The results of FTIR spectra suggested that some new adsorption peaks appeared after SPA and HEPA treatment, which inferred that HEPA and SPA might adsorb onto the minerals with the formation of new complexes.

3.4 DFT calculation

The phosphonic acid solved in water may exist in three forms: molecular form, monoanion form and dianion form, as shown in Scheme 1. The proportion of different forms was depended on the ionization equilibriums and had an important effect on the reaction between collectors and mineral surfaces. Different forms of HEPA and SPA were calculated by DFT calculation to study the effect of collector structure on the reaction. The optimized geometries of phosphonic acid molecular and their ionic species were listed in Table 1.



Scheme 1 Ionization of phosphonic acid in aqueous solutions

3.4.1 Structure details of SPA and HEPA

The selected structure parameters of bond length and bond angle of HEPA and SPA were listed in Table 2, while the numbering scheme was described in Fig. 6.

Based on the data in Table 2, the P—O and P=O bond length and O—P—O angle of HEPA were not different from those of SPA. The bond lengths of these two collectors varied with the ionization degree: the length of P=O bond increased but the length difference between P—O bond and P=O bond decreased with the increase of ionization degree. The reason was attributed to the formation of a big conjugative π bond by the P=O bond and the ionization O atoms.

However, the C—P bond in HEPA species was longer than that in SPA. The results in Table 2 suggested that the C—P bonds in SPA were respectively 1.778, 1.808 and 1.835 Å, which were shorter than 1.851, 1.872 and 1.914 Å in HEPA correspondingly. It may be due to the effect of alkyl group. The conjugative effect between phenyl group and ethylene made the C5 atom of SPA owned much more electronics (Table 3), enhancing the interaction between C5 and P atoms. Therefore, the C—P bond of SPA was stronger and shorter than that of HEPA.

In terms of bond angle, the big conjugative π bond formed by the P=O bond and the ionization O atoms resulted in an enlargement of O1—P—O2 bond angle for

Table 1 Optimized geometries of phosphonic acid molecular and their ionic species

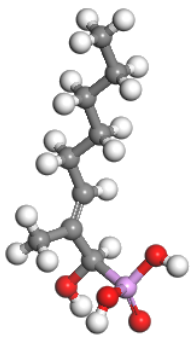
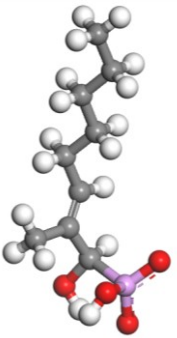
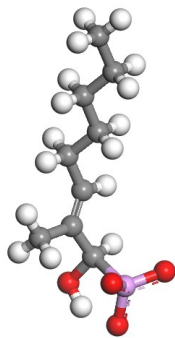
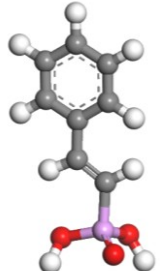
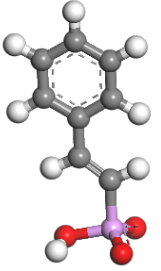
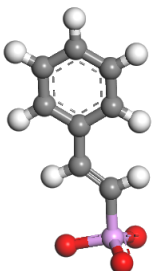
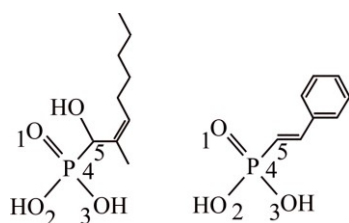
| Collector | Molecule | Monoanion | Dianion |
|-----------|---|---|---|
| HEPA |  |  |  |
| SPA |  |  |  |

Table 2 Selected optimized geometrical parameters for HEPA and SPA

| Collector | State | Bond length/Å | | | | Bond angle/(°) | | |
|-----------|-----------|---------------|-------|-------|-------|----------------|---------|---------|
| | | P=O1 | P—O2 | P—O3 | C—P | O1—P—O2 | O1—P—O3 | O2—P—O3 |
| SPA | Molecule | 1.498 | 1.616 | 1.624 | 1.778 | 115.349 | 114.018 | 102.159 |
| | Monoanion | 1.521 | 1.517 | 1.664 | 1.808 | 120.129 | 108.915 | 105.959 |
| | Dianion | 1.551 | 1.55 | 1.546 | 1.835 | 112.991 | 113.855 | 113.918 |
| HEPA | Molecule | 1.499 | 1.612 | 1.625 | 1.851 | 117.563 | 113.372 | 101.977 |
| | Monoanion | 1.529 | 1.513 | 1.666 | 1.872 | 121.681 | 108.138 | 105.679 |
| | Dianion | 1.569 | 1.544 | 1.544 | 1.914 | 113.035 | 113.670 | 113.901 |

**Fig. 6** Numbering scheme of HEPA and SPA

monoanions. All the bond angle of O—P—O of dianions approximated 113°.

3.4.2 Mulliken charges of SPA and HEPA

The Mulliken charge analysis results of SPA and HEPA species were shown in Table 3. The data indicated that the O1 atom in P=O owned more electronics compared with the O2 and O3 atoms in P—O bond for both of these two molecules. However, the charge difference between O1 and O2 became insignificant for both SPA and HEPA monoanions. Above all, the negative

Table 3 Mulliken charge of atoms in HEPA and SPA

| Collector | State | O1 | P4 | O2 | O3 | C5 |
|-----------|-----------|--------|-------|--------|--------|--------|
| SPA | Molecule | -0.779 | 1.574 | -0.640 | -0.654 | -0.514 |
| | Monoanion | -0.871 | 1.459 | -0.866 | -0.704 | -0.503 |
| HEPA | Molecule | -0.783 | 1.547 | -0.645 | -0.636 | -0.217 |
| | Monoanion | -0.884 | 1.443 | -0.861 | -0.693 | -0.224 |
| | Dianion | -0.967 | 1.343 | -0.954 | -0.936 | -0.226 |

charges of SPA and HEPA monoanions were mainly focused on the O1 and O2 atoms, suggesting that these two atoms were of electron-donating center, i.e., chemical reactivity center. In addition, the charges of O1, O2 and P atoms in HEPA monoanion were respectively -0.884, -0.861 and 1.433, while the charges for corresponding atoms in SPA were -0.871, -0.866 and 1.459. It was obvious that the group “O=P—O” in

HEPA monoanions had a negative charge of -0.312 , which was more negative than -0.278 in SPA monoanions. Hence, HEPA monoanions owned stronger electron-donating ability compared with SPA monoanions. HEPA and SPA dianions had more negative charges, meaning that these two dianions should have strong electrostatic repulsion with mineral surfaces.

3.4.3 Frontier molecular orbital analysis

According to the Klopman perturbation energy equation of chemical reactivity, which incorporates the effect of an external electrostatic field in both charge and orbital contributions, the energy of reaction is primarily determined by the electrostatic effect and the frontier molecular orbital (FMO) of reactants [30,31]. The electrostatic effect is proportional to the net charge at reactive center of reactants, which has been discussed in Refs. [31,32]. In the reaction between minerals and collectors, the HOMO of collectors donates electrons to the LUMO of mineral, while the HOMO of minerals back donates electrons to the LUMO of collectors if the metal atoms in mineral surface have rich d-orbital electrons [17]. However, in this study, the Sn was main group element. There were not rich d-orbital electrons in the LUMO of Sn atoms, resulting in the fact that the LUMO of collector has little impact on the interaction. Hence, only the HOMO of collectors was discussed. The collector which owns the higher HOMO value had a more powerful electrons-donating ability and was easier to react with the metal atoms in minerals surfaces.

The calculated FMO eigenvalues of HEPA and SPA were given in Table 4. It can be observed that both the molecular and monoanion species of HEPA had higher HOMO values than corresponding species of SPA. Hence the molecular and monoanion of HEPA owned higher activity than corresponding species of SPA. The results are consistent with the flotation experimental observation that HEPA had stronger collecting ability compared with SPA. While the comparison between SPA dianions and HEPA dianions was opposite to above.

3.5 Flotation behavior of HEPA

According the solution chemistry, the species distribution of molecular was primarily determined by its ionization constant and the pH value of solution environment. The ionization constants of SPA have been reported in many previous studies. However, the ionization constants of HEPA have not been reported yet.

The ionization constants of HEPA calculated by ilab of ACD/labs were 1.7 for pK_{a1} and 6.6 for pK_{a2} , respectively. The species distribution diagram of HEPA as a function of solution pH is shown in Fig. 7.

To expound the mechanism responsible for adsorption of HEPA on cassiterite surface, the dependence of the flotation recovery, zeta potential and the species distribution diagram of HEPA were plotted in Fig. 7. The variations in flotation recovery, zeta potential and the species distribution diagram of HEPA with increasing pH could be divided into four parts for HEPA solution.

At $pH < 1.7$, molecule species were the dominant component in solution. The basal planes of cassiterite were positively charged. The minority of HEPA monoanions in solution were adsorbed onto the mineral surface by electronic effect and chemical adsorption. Hence, the flotation recovery of cassiterite was not high.

In the pH region of 1.7–6.6, monoanions were the dominant component of HEPA in solution. Meanwhile, the flotation recovery was also relative preferable in these range. These results inferred that monoanions of HEPA were the functional component for flotation. The adsorption of HEPA made zeta potentials negative shift. When pH value was around 4.0, the proportion of dominant component monoanions and flotation recovery reached the peak. Since the cassiterite was negatively charged in the pH region of 3.6–6.6, the adsorption of HEPA monoanions onto cassiterite surfaces have to overcome the electrostatic repulsion, which further demonstrated that adsorption behavior of HEPA onto the cassiterite surface was primarily attributed to chemisorption. The chemistry interaction of FMO was stronger than the electrostatic effect.

In the pH range from 6.6 to 9.1, the proportion of dianions increased with the increase of pH, in contrast to that, the monoanion concentration descended. The charge of dianions was more negative than that of monoanions, resulting in a stronger electrostatic repulsion. Therefore, the dianions could hardly adsorb onto mineral surfaces, hence the adsorption amount and flotation recovery started to decrease.

When pH values were over 9.1, the monoanions of HEPA nearly disappeared in solution. The negative charge of normal mineral surface increased. The electrostatic repulsion further increased. Flotation recovery declined rapidly to the bottom in this region.

Table 4 Calculated frontier orbital eigenvalues for HEPA and SPA

| Collector | Molecule | | Monoanion | | Dianion | |
|-----------|----------|----------|-----------|----------|----------|----------|
| | HOMO | LUMO | HOMO | LUMO | HOMO | LUMO |
| SPA | -0.22090 | -0.09463 | -0.19513 | -0.07442 | -0.14604 | -0.06061 |
| HEPA | -0.20956 | -0.03203 | -0.18959 | -0.01456 | -0.15134 | 0.00107 |

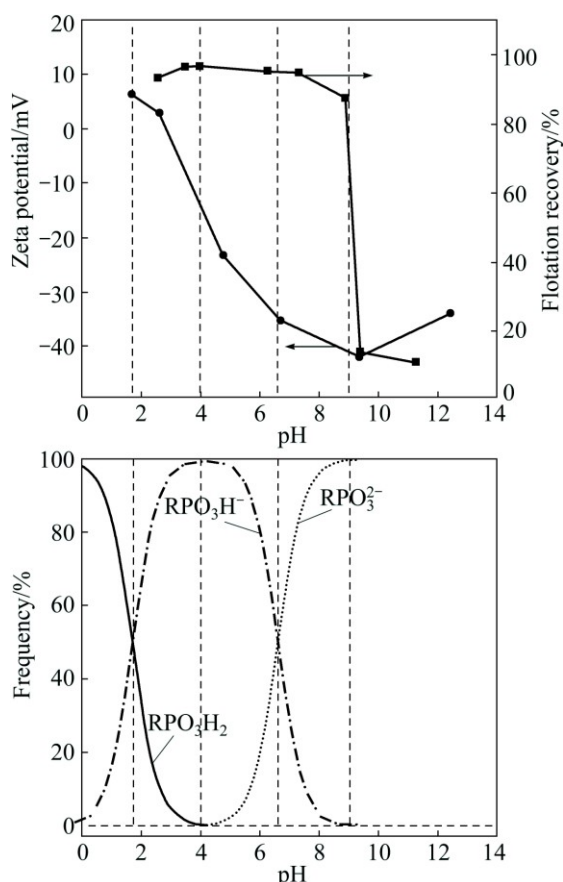


Fig. 7 Dependence of flotation recovery, zeta potential and species distribution diagram of HEPA

3.6 Adsorption mechanism of HEPA

The above discussion demonstrated that monoanion of HEPA was the functional component of flotation and HEPA interacted with mineral surfaces through chemical adsorption. The former report by KUYS and ROBERTS [27] had suggested that SPA adsorbed onto the cassiterite surface by a chemisorption process of the O atoms of phosphate bonding with the metal atoms on the cassiterite surfaces. LI et al [13] pointed out that HPA reacted with Sn species by formation of Sn—O—P and Sn—P bonds.

The DFT calculation results showed that O1 and O2 atoms were of the active center in HEPA monoanions. Therefore, we proposed the possible chemisorption process and bonding configuration of HEPA monoanion with Sn species on cassiterite surfaces in acid conditions, as illustrated in Fig. 8 and Fig. 9.

In these reactions, step 1 was the key step, which has been demonstrated by FARROW et al [33] and KUYS and RORERTS [27]. Based on these reports, the monoanion of phosphonic acid undergoes slow ion exchange and reacts with the surface hydroxyl groups of cassiterite, resulting in the formation of monodentate complexes in step 1. Simultaneously, the other P—OH of HEPA reacts with another hydroxyl groups of cassiterite,

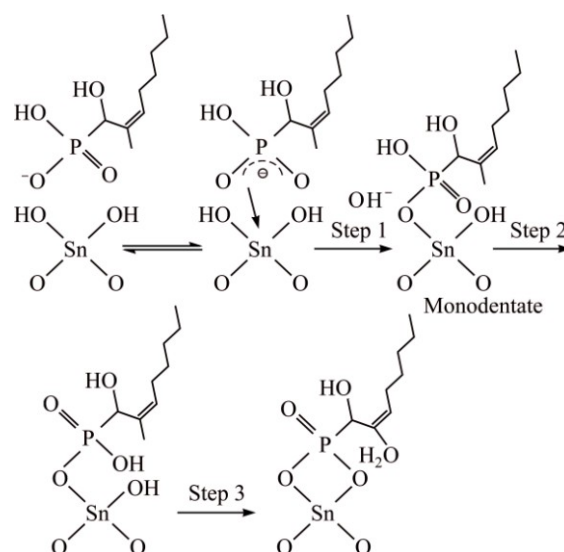


Fig. 8 Possible chemisorption process of HEPA onto cassiterite surface

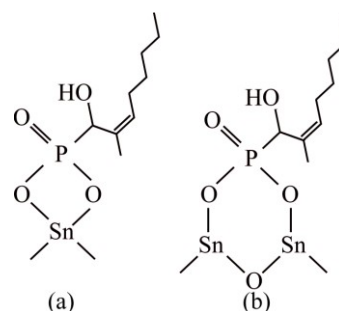


Fig. 9 Bonding configuration of bidentate (a) and binuclear (b)

giving out a H_2O molecular, followed by rapid formation of a bidentate complex or a binuclear complex (see Fig. 9) [27]. Whatever, the monodentate complexes that formed by monoanions of phosphonic acid reacting with the Sn species on mineral surfaces are the foremost intermediates in these reactions.

To compare the reaction ability of HEPA with that of SPA, the binding models of monodentate complexes formed by collector monoanions and cassiterite surfaces were simulated and calculated. The optimized models were illustrated in Fig. 10 and the values of binding energy were calculated as follows:

$$\Delta E = E_{a/b} - (E_{HEPA/SPA} + E_{SnO_2}) \quad (1)$$

where $E_{a/b}$ is the total energy of models a or b, $E_{HEPA/SPA}$ is the energy of phosphonic acid monoanions, and E_{SnO_2} is the energy of cassiterite surface.

The calculation results indicated the binding energies of HEPA and SPA were respectively -75.35 and -56.28 kJ/mol, which revealed that the reactive process of HEPA or SPA with Sn species might take place favorably since both of these binding energies were negative. Additionally, the binding energy of HEPA

model (a) was more negative than that of SPA model (b), leading to the fact that HEPA exhibited higher reaction activity to cassiterite than SPA. The theoretically obtained results by DFT calculation are in highly accordance with those previously experiment results.

All these results demonstrated that the mechanism of HEPA adsorption onto cassiterite surface was a chemisorption process and the HEPA had a better collecting ability to cassiterite than SPA. However, the mechanism of HEPA rapidly collecting the cassiterite without frother was still unknown.

3.7 Flotation mechanism of HEPA

The flotation tests have demonstrated that HEPA had a much higher surface activity to cassiterite than SPA. The surfaces activities of collectors have been proved to have an important relationship with the surface tension of molecules [34,35]. According to the calculation results provided by ilab/ACD labs, the surface tensions of HEPA and SPA were 47.8×10^{-3} N/m and 63.7×10^{-3} N/m, respectively.

The HEPA owned much lower surface tension than SPA. Therefore, HEPA was more efficient than SPA in decreasing the air–water interfacial tension, which may be attributed to the steric effect of the alkyl group [35]. There are many reports about the relationship between the molecular structure and the surface tension [36,37]. The structures of HEPA and SPA have been discussed in the DFT research. The longer C—P bond and hydrocarbon group offer more significant contributions in inducing hydrophobicity when HEPA adsorbed on cassiterite interfaces.

When phosphonic acid collectors were added to the solution, the polar group of collectors adsorbed onto cassiterite surfaces and the hydrophobic group attached to air bubbles [38]. Since HEPA was more effective in reducing the air–water interfacial tension than SPA, the resistance to bubble coalescence and the stability of froth formed by HEPA were better than that of SPA [39,40]. Hence, HEPA showed great flotation efficiency to cassiterite. The flotation adsorption model was shown in Fig. 11. However, SPA molecules which have a high

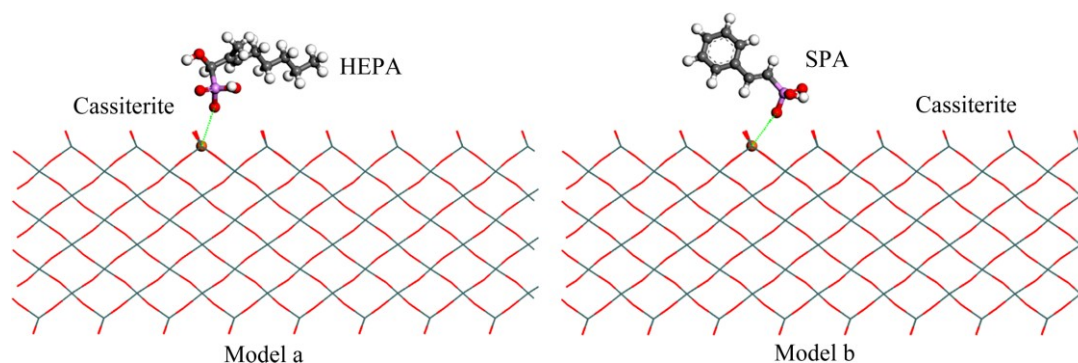


Fig. 10 Optimized binding model of collector monoanions and cassiterite surface

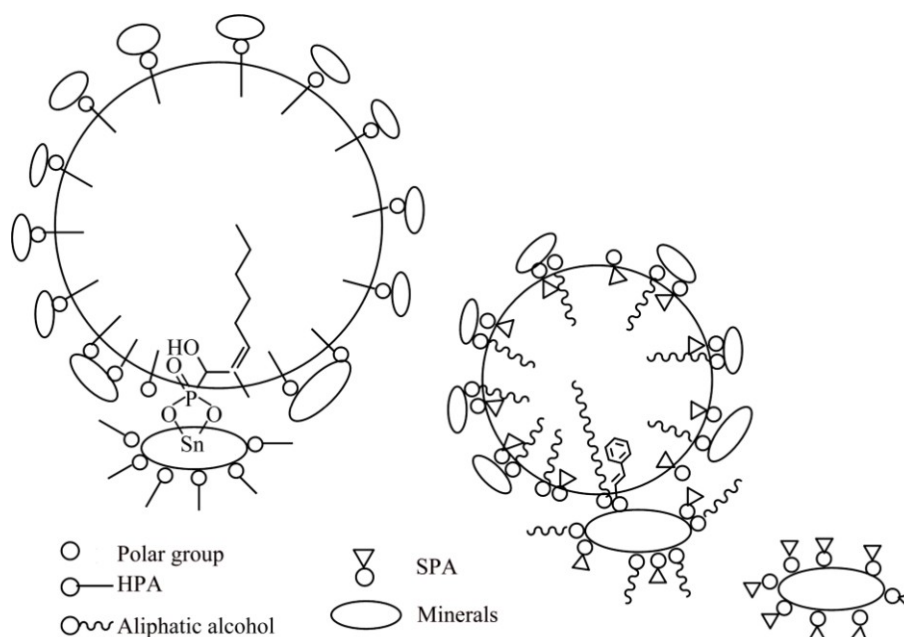


Fig. 11 Flotation adsorption models of HEPA and SPA on cassiterite surface

surface tension show a bad flotation performance. With the addition of aliphatic alcohol, the frother molecules which have a low surface tension make intermolecular association with SPA molecules, resulting in the reduction of air–water interfacial tension. Therefore, minerals were attached to the bubbles and collected successfully (Fig. 11) by foam flotation.

4 Conclusions

1) The flotation results indicated that HEPA presented stronger collecting power to cassiterite compared with SPA, and the flotation recovery maintained above 90% over the pH region of 2–9 when HEPA concentration was 50 mg/L. While the recovery was around 80% over the pH range of 2–7 when 50 mg/L SPA was used in the presence of frother 2# oil.

2) HEPA and SPA collectors adsorbed onto the cassiterite surfaces by a chemisorption process were demonstrated by FTIR spectra and zeta potential measurements. The solution chemistry analysis suggested that the active principle of flotation was phosphonic acid monoanion, which overcame the electrostatic repulsion and formed a strong chemisorption with cassiterite. HEPA showed a better affinity to cassiterite than SPA.

3) HEPA monoanions owned more negative charge and higher HOMO values than SPA monoanions, HEPA more easily donated electrons to the metal atoms of cassiterite surfaces. The bond configuration models of collectors with cassiterite surface were established and the binding energy of model was also calculated. The binding energy E_{HEPA} was more negative than E_{SPA} , further demonstrating that HEPA exhibited a stronger collecting power to cassiterite compared with SPA. The longer C–P bond and hydrocarbon group of HEPA made HEPA own less surface tension than SPA, resulting in the fact that HEPA can float out cassiterite without 2# oil. The theoretical results showed an excellent agreement with the flotation tests, FTIR spectra studies and zeta potential measurements.

Acknowledgements

The authors are thankful to the 12th Five-year plan of national scientific and technological program of China (2013AA064102). The authors would like also thank to ilab of ACD/labs for providing supports. A special gratitude is expressed to Professor Hong ZHONG, Professor Guang-yi LIU and Professor Shuai WANG of Central South University for their kindly help.

References

[1] GRUNER H, BILSING U. Cassiterite flotation using styrene

phosphonic acid to produce high-grade concentrates at high recoveries from finely disseminated ores-comparison with other collectors and discussion of effective circuit configurations [J]. *Minerals Engineering*, 1992, 5(3–5): 429–434.

- [2] DECUYPER J, SALAS A. Flotation of cassiterite [C]//Proceedings of International Tin Symposium. La Pez, Bolivia, 1977.
- [3] SENIOR G, POLING G. The chemistry of cassiterite flotation [C]//SOMASUNDARAN P Ed. *Advances in Mineral Processing*. Littleton: SME/AIME, 1986: 229–254.
- [4] SREENIVAS T, MANOHAR C. Investigations on the collector reagent development for the recovery of cassiterite from the gravity tails of a low grade Indian tin ore [J]. *Mineral Processing and Extractive Metallurgy Review*, 1998, 19: 461–479.
- [5] BULATOVIC, SRDJAN M. Handbook of flotation reagents: Chemistry. Theory and Practice, Vol. 2. Flotation of Gold, PGM and Oxide Minerals [M]. Amsterdam: Elsevier, 2010.
- [6] ARBITER N. Beneficiation of cassiterite ores by froth flotation: British Patent No. 110643 [P]. 1968–04–24.
- [7] KHANGAONKAR P R, KAMARUDIN H. Studies on the cassiterite sulphosuccinamate flotation system [J]. *International Journal of Mineral Processing*, 1994, 42: 99–110.
- [8] QIN Wen-qin, XU Yang-bo, LIU Hui, REN Liu-ying, YANG Cong-ren. Flotation and surface behavior of cassiterite with salicylhydroxamic acid [J]. *Industrial and Engineering Chemistry Research*, 2011, 50(18): 10778–10783.
- [9] SREENIVAS T, PADMANABHAN N P H. Surface chemistry and flotation of cassiterite with alkyl hydroxamates [J]. *Colloids and Surfaces A: Physicochemical and Engineering Aspects*, 2002, 205: 47–59.
- [10] ANGADI S I, SREENIVAS T, JEON H S, BAEK S H, MISHRA B K. A review of cassiterite beneficiation fundamentals and plant practices [J]. *Minerals Engineering*, 2015, 70: 178–200.
- [11] COLLINS D N, KIRKUP L, DAVEY M N, ARTHUR C. Flotation of cassiterite: Development of a flotation process [J]. *Transactions of the Institution of Mining and Metallurgy*, 1968, 77: 1–13.
- [12] CHENG Jian-guo, ZHU Jian-guang. A study of the collecting performances and adsorption mechanism of alkylphosphorous ester on cassiterite [J]. *Nonferrous Metals*, 1986, 38(4): 37–43. (in Chinese)
- [13] LI Fang-xu, ZHONG Hong, ZHAO Gang, WANG Shuai, LIU Guang-yi. Flotation performances and adsorption mechanism of α -hydroxyoctylphosphinic acid to cassiterite [J]. *Applied Surface Science*, 2015, 353: 856–864.
- [14] LIN Qiang, ZHUO Zi-yun, JI Gan-fang, WANG Dian-zuo. Synthesis of monoalkyl phenyl-phosphonates and their structure-reactivity relationship as collectors of nonsulfides [J]. *Journal of Central South Inst Min Metall*, 1989, 20(4): 367–374. (in Chinese)
- [15] ZIEGLER T. Approximate density functional theory as a practical tool in molecular energetics and dynamics [J]. *Chemical Reviews*, 1991, 91: 651–667.
- [16] KOHN W, BECKE A D, PARR R G. Density functional theory of electronic structure [J]. *Journal of Physical Chemistry*, 1996, 100: 12974–12980.
- [17] ZHAO Gang, ZHONG Hong, QIU Xian-yang, WANG Shuai, GAO Yu-de, DAI Zi-lin, HUANG Jian-ping, LIU Guang-yi. The DFT study of cyclohexyl hydroxamic acid as a collector in scheelite flotation [J]. *Minerals Engineering*, 2013, 49: 54–60.
- [18] FEN Jiao, QIN Wen-qing, LIU Rui-zeng, WANG Xing-jie. Adsorption mechanism of 2-mercaptobenzothiazole on chalcopyrite and sphalerite surfaces: Ab initio and spectroscopy studies [J]. *Transactions of Nonferrous Metals Society of China*, 2015, 25(7): 2388–2397.
- [19] ZHAO Ya-ying, TAO Fu-ming, ZENG E Y. Theoretical study of the quantitative structure-activity relationships for the toxicity of

- dibenzo-p-dioxins [J]. Chemosphere, 2008, 73: 86–91.
- [20] ZHAO Cui-hua, CHEN Jian-hua, LI Yu-qiong, CHEN Ye, LI Wei-zhou. First-principle calculations of interaction of O₂ with pyrite, marcasite and pyrrhotite surfaces [J]. Transactions of Nonferrous Metals Society of China, 2016, 26(2): 519–526.
- [21] OVIEDO J M, GILLAN J. Energetics and structure of stoichiometric SnO₂ Surfaces studied by first-principles calculations [J]. Surface Science, 2000, 463: 93–101.
- [22] ALBOUY D, BRUN A, MUNOZ A. New (α -hydroxyalkyl) phosphorus amphiphiles: Synthesis and dissociation constants [J]. Journal of Organic Chemistry, 1998, 63(21): 7223–7230.
- [23] ZHONG Hong, LI Fang-xu, WANG Shuai, HUANG Zi-qiang, LIU Guang-yi, CAO Zhan-fang. The synthesis and application method of α -hydroxy-unsaturated alkyl phosphonic acids: Chinese Patent CN 103613614 A [P]. 2014–03–05.
- [24] ZHANG Qin-fa, TIAN Zhong-cheng. Action mechanism of the flotation of cassiterite using mixed toluene-arsenic acid [J]. Mining and Metallurgical Engineering, 1989, 9(1): 19–21. (in Chinese)
- [25] ZENG Qing-hua, ZHAO Hong. The flotation chemistry of cassiterite [J]. Metallic Ore Dressing Abroad, 1997, 3: 6–14. (in Chinese)
- [26] PENG Wen-shi, LIU Gao-kui. IR spectrum atlas of mineral [M]. Beijing: Science Press, 1982: 115. (in Chinese)
- [27] KUYS K J, ROBERTS N K. In situ investigation of the adsorption of styrene phosphonic acid on cassiterite by FTIR-ATR [J]. Colloids and Surfaces, 1987, 24: 1–17.
- [28] WANG K P, LIU Q. Adsorption of phosphorylated chitosan on mineral surfaces [J]. Colloids and Surfaces A: Physicochemical and Engineering Aspects, 2013, 436: 656–663.
- [29] CHEN G, TAO D, REN H, JI F, QIAO J. An investigation of niobite flotation with octyldiphosphonic acid as collector [J]. International Journal of Mineral Processing, 2005, 76: 111–122.
- [30] LIU Guang-yi, ZHONG Hong, TAI Ta-gen, XIA Liu-yin. Flotation separation of Cu/Fe sulfide minerals by ethoxycarbonyl thiourea under middle alkaline conditions [J]. The Chinese Journal of Nonferrous Metals, 2009, 19(2): 389–396. (in Chinese)
- [31] LIU Guang-yi, XIAO Jing-jing, ZHOU Di-wen, ZHONG Hong, PHILLIP C, XU Zheng-he. A DFT study on the structure-reactivity relationship of thiophosphorus acids as flotation collectors with sulfide minerals: Implication of surface adsorption [J]. Colloids and Surfaces A: Physicochemical and Engineering Aspects, 2013, 434: 243–252.
- [32] LIU Guang-yi, ZENG Hong-bo, LU Qing-ye, ZHONG Hong, PHILLIP C, XU Zheng-he. Adsorption of mercaptobenzoheterocyclic compounds on sulfide mineral surfaces: A density functional theory study of structure-reactivity relations [J]. Colloids and Surfaces A: Physicochemical and Engineering Aspects, 2012, 409: 1–9.
- [33] FARROW J B, HOUCHEIN M R, WARREN L J. Mechanism of adsorption of organic acids on stannic oxide [J]. Colloids and Surface, 1988–1989, 34(3): 255–269.
- [34] CHANG C H, FRANCES E I. Adsorption dynamics of surfactants at the air/water interface: A critical review of mathematical models, data, and mechanisms [J]. Colloids and Surfaces A: Physicochemical and Engineering Aspects, 1995, 100: 1–45.
- [35] PROSSER A J, FRANCES E I. Adsorption and surface tension of ionic surfactants at the air–water interface: Review and evaluation of equilibrium models [J]. Colloids and Surfaces A: Physicochemical and Engineering Aspects, 2001, 178: 1–40.
- [36] SHAFRIN E G, ZISMAN W A. Constitutive relations in the wetting of low energy surfaces and the theory of the retraction method of preparing monolayers [J]. Journal of Physical Chemistry, 1960, 64(5): 519–524.
- [37] ZISMAN W A. Relation of the equilibrium contact angle to liquid and solid constitution [J]. Advances in Chemistry Series, 1964, 43(1): 1–51.
- [38] ZHANG Wei. Evaluation of effect of viscosity changes on bubble size in a mechanical flotation cell [J]. Transactions of Nonferrous Metals Society of China, 2014, 24(9): 2964–2968.
- [39] REN Liu-yi, ZHANG Yi-min, QIN Wen-qing, BAO Shen-xu, WANG Jun. Collision and attachment behavior between fine cassiterite particles and H₂ bubbles [J]. Transactions of Nonferrous Metals Society of China, 2014, 24(2): 520–527.
- [40] SRDJAN M B. Handbook of flotation reagents: Chemistry, theory and practice: Flotation of sulfide ores [M]. Amsterdam: Elsevier Science & Technology Books, 2007.

1-羟基-2-甲基-2-烯辛基膦酸对锡石的浮选行为及吸附机理

谭鑫^{1,2}, 何发钰³, 尚衍波², 印万忠¹

1. 东北大学 资源与土木工程学院, 沈阳 110819;

2. 北京矿冶研究总院 矿物加工科学与技术国家重点实验室, 北京 102628;

3. 中国五矿集团总公司, 北京 100010

摘要: 采用纯矿物浮选实验、动电位测试、红外光谱检测以及密度泛函理论计算研究了 1-羟基-2-甲基-2-烯辛基膦酸(HEPA)对锡石的浮选行为及吸附机理。浮选实验结果表明, 相比苯乙烯膦酸(SPA), HEPA 具有出更强的捕收性能。当 HEPA 浓度为 50 mg/L 时, 在 pH 2–9 范围内锡石回收率都保持在 90%以上。动电位测试和红外光谱检测结果表明, HEPA 在锡石表面的吸附主要是通过 HEPA 单阴离子与锡石表面的锡原子形成化学吸附。密度泛函计算结果表明, HEPA 单阴离子比 SPA 单阴离子具有更高的 HOMO 能量和对锡石更强的吸附力, 这为浮选实验和动电位测试中 HEPA 的更强捕收力提供了有力证明。

关键词: 1-羟基-2-甲基-2-烯辛基膦酸(HEPA); 锡石; 吸附; 浮选; 密度泛函理论

(Edited by Yun-bin HE)